Histology-directed MALDI mass spectrometry for the diagnostic pathology

Hark Kyun Kim, In-Hoo Kim*
Research Institute & Hospital, National Cancer Center, 323 Ilsan-ro, Goyang, Gyeonggi 410-769, Republic of Korea

ABSTRACT

With the advent of targeted agents, it has become clinically important to distinguish histologic types of non-small cell lung cancers (NSCLCs) using biopsy samples. We investigated whether direct tissue matrix-assisted laser desorption/ionization (MALDI) mass spectrometry (MS) analysis on lipid may classify histology of NSCLCs. Twenty-one pairs of frozen, resected NSCLCs were analyzed using histology-directed, MALDI MS. 2,5-dihydroxybenzoic acid/α-cyano-4-hydroxycinnamic acid were manually deposited on areas of each tissue section enriched in epithelial cells to identify lipid profiles, and mass spectra were acquired using a MALDI-time of flight instrument. Squamous cell carcinomas and adenocarcinomas, two major histologic types of NSCLC, were found to have different lipid profiles. Discriminatory lipids correctly classified the histology of 80.4% of independent NSCLC surgical tissue samples (41 out of 51) in validation set, suggesting that lipid profiles can classify NSCLCs according to the histologic type. We also found that protein and lipid MALDI MS profiles can classify 30 breast cancers according to the intrinsic subtypes. Immunohistochemistry-defined, luminal, HER2+, and triple-negative tumors demonstrated different protein and lipid profiles, as evidenced by cross validation P values < 0.01. Discriminatory proteins and lipids classified tumors according to the intrinsic subtype with median prediction accuracies of 80.0-81.3% in 100 random test sets. Potential advantages of this label-free approach may include small tissue requirement, relatively rapid procedure, and low reagent cost. Day-to-day variation of this technology is also acceptable, with the Pearson correlation of 0.95. Taken together, these results suggest the possible clinical utility of histology-directed, lipid and protein MALDI MS.

Key words: MALDI, histology, cancer

1.BACKGROUND

Matrix-assisted laser desorption/ionization mass spectrometry (MALDI MS) has been demonstrated to be useful for direct molecular profiling of common cancers[1]. In this approach, sinapinic acid is deposited on tumor-rich area of tissue cryosections, and mass spectra are obtained. The resulting spectra are composed primarily of singly charged ions of proteins present in tumor-rich area. Hence, this approach captures relatively pure tumor cell-specific signals, and requires less tissue amount than tissue lysate-based proteomics technologies. Recent advances in MALDI MS and the related development of effective matrices made it possible to directly probe tissues to profile lipid composition and distribution[2].

Current histopathologic methods have some limitations in histopathologic classification of small biopsy samples. In non-small cell lung cancers (NSCLCs), for example, the accuracy and reliability of morphologic subclassification alone in small biopsies are low, and approximately 25% of bronchoscopic biopsies cannot be subtyped based on morphology alone. Addition of the immunohistochemistry panels classifies 80-90% of these NSCLC cases, with 10-20% of cases remaining unclassified for the histologic subtype[3]. Thus, there is the unmet need for sensitive and specific biomarkers for histopathologic diagnosis of NSCLCs.

*ihkim@ncc.re.kr; phone +82 31 920-1503; fax +82 31 920-1511

Nanosystems in Engineering and Medicine, edited by Sang H. Choi, Jin-Ho Choy, Uhn Lee, Vijay K. Varadan,
Proc. of SPIE Vol. 8548, 854823 · © 2012 SPIE · CCC code: 1605-742/12/$18 · doi: 10.1117/12.1000001

2.DATA

To explore whether lipid MALDI MS profiles may be more useful than conventional protein MALDI MS profiles in histopathologic diagnosis of NSCLCs, 21 pairs of frozen, resected NSCLCs and adjacent normal tissue samples were analyzed. 2,5-dihydroxybenzoic acid / α-cyano-4-hydroxycinnamic acid (DHB/CHCA) were manually deposited on areas of each tissue section enriched in epithelial cells to identify lipid profiles, and mass spectra were acquired using a MALDI-time of flight instrument (TOF). In 4 out of 21 lung cancer samples (19%), the entire sample had >50% of tumor nuclei. In the remaining 17 samples (81%), the pathologist marked the H&E-stained consecutive cryosection slide at tumor-rich (>50% of tumor nuclei) area, and care was taken to deposit the DHB/CHCA matrix within the boundary of marked tumor-rich area. The average MALDI MS spectra were composed of 3 to 5 individual measurements for cancer samples (with a median value of 3), and 3 to 5 individual measurements for adjacent normal samples (with a median value of 4). The individual measurements were averaged in order to minimize intra-sample variability. Post-spectral processing identified 144 features (78 and 66 for positive and negative modes, respectively) across the entire mass range for all of the samples studied. This analysis revealed that squamous cell carcinomas and adenocarcinomas have different lipid profiles. Eleven lipid MALDI peaks, which were differentially expressed between squamous cell carcinomas and adenocarcinomas in this training set, correctly classified the histology of 80.4% of NSCLC surgical tissue samples (41 out of 51) in validation set. Fig 1 graphically displays principal component analysis plots of NSCLC samples in training and validation sets, based on all MALDI MS peaks acquired at the m/z ranging from 500 to 1,200.

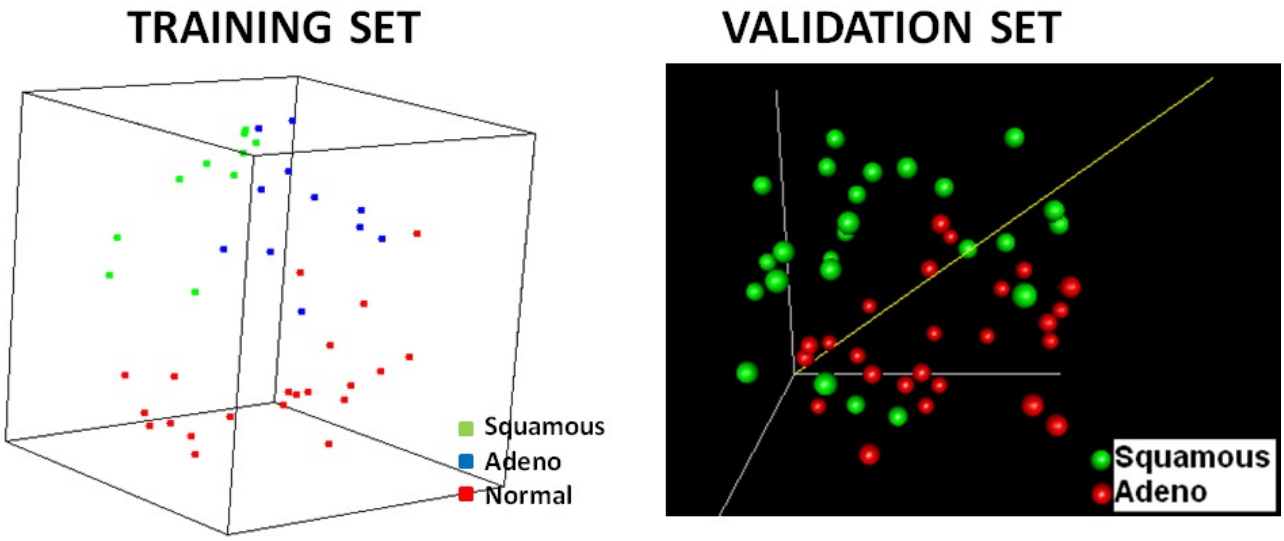

Fig 1. The left panel shows a principal component analysis plot for 21 pairs of adjacent normal (*shown in red*) and lung cancer tissue samples (10 squamous cell carcinomas (*shown in green*) and 11 adenocarcinomas (*shown in blue*)) in the training set, which graphically represents 1-correlation distances among samples, based 144 MALDI MS peaks detected at the m/z range 500-1,200 (78 and 66 peaks detected in positive and negative ion modes, respectively). The right panel shows a principal component analysis plot for the validation set (26 squamous cell carcinomas (*shown in green*) and 25 adenocarcinomas (*shown in red*)), based all lipid MALDI MS peaks. Figure is reproduced from our previous article, Ref. #4.

Classification power of these discriminatory lipids was further validated in imaging MALDI MS analysis on bronchoscopic biopsy samples, which demonstrated their differential expression in cancer cells between squamous cell carcinomas and adenocarcinomas (Fig 2).

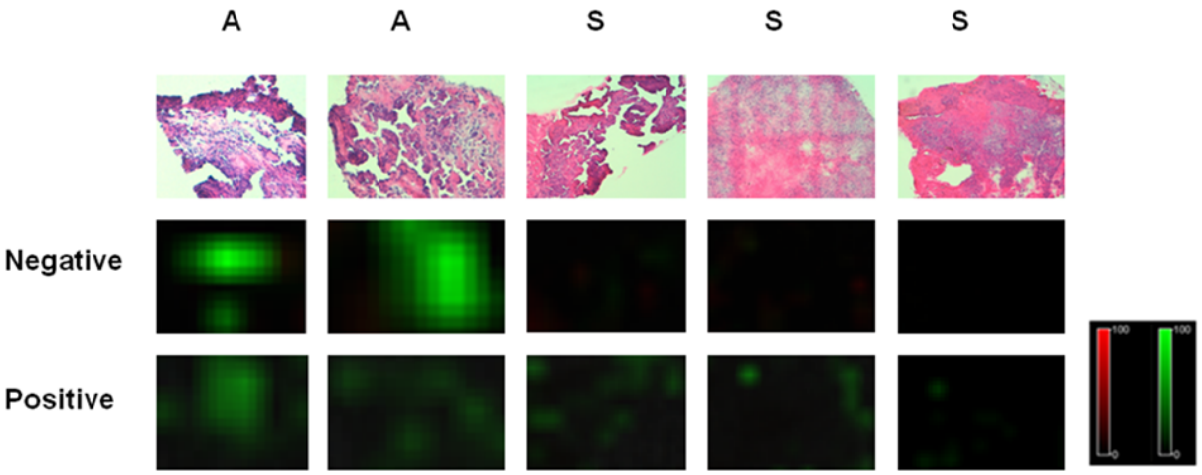

Fig 2. Mass spectrometry images of the same discriminatory peaks as (A) generated based on the sum of intensity of individual peak. Intensities of peaks overexpressed in squamous cell carcinoma surgical samples (I of (A)) and peaks overexpressed in adenocarcinoma surgical samples (II of (A)) are graphically displayed in red and green colors, respectively, according to scale bars shown at the bottom right. Peaks overexpressed in surgical adenocarcinoma surgical samples (*shown in green*) showed coordinated overexpression in cancer cells of adenocarcinoma biopsy samples (denoted as "A"), while peaks overexpressed in surgical squamous cell carcinoma samples (*shown in red*) showed coordinated overexpression in squamous cell carcinoma biopsy samples (denoted as "S"). Scale bars for the relative peak intensity are shown at bottom right. Figure is reproduced from our previous article, Ref. #4.

We also asked the same question using direct tissue MALDI analysis for 50 lung cancer bronchoscopic biopsy samples and 7 adjacent normal tissue samples. Among 43 NSCLC bronchoscopic biopsy samples available, there were 7 adenocarcinomas and 30 squamous cell carcinomas. When we estimated the predictive power of discriminatory peaks in random training-to-test partitions, the median prediction accuracy of the best predictor in test sets (at feature selection $P<0.05$) was 83.3% in 100 random training-to-test partitions. Therefore, both lipid and protein MALDI MS profiles can classify NSCLCs according to histologic subtype.

We then asked whether combined lipid and protein MADLI MS profiles may better capture biologic information from clinical cancer specimens than conventional protein MALDI MS profiles. Using colon cancer specimens, we performed separate class prediction analyses on protein and lipid MALDI profile datasets. At a feature selection $P<0.001$, the median class prediction accuracy of the best protein predictor in random test sets was 92.3% (12 out of 13 pairs), in 100 random training-to-test partitions. The median class prediction accuracy of the best lipid predictor was also 92.3% (12 out of 13 pairs). When the same analysis was performed on the combined protein and lipid MALDI profile dataset, the median class prediction accuracy of the best predictor in test sets was 100% (13 out of 13 pairs). Thus, the addition of lipid MALDI profiles to conventional protein MALDI profiles offered better distinction between cancer and normal epithelium. When additional 13 pairs of cancer and adjacent normal samples were used to validate the cancer-specific lipid MALDI profiles, the best predictor with peaks differentially expressed between 23 pairs of cancer and adjacent normal samples of the training set correctly predicted 100% of validation set samples (13 out of 13 pairs). Phosphatidylcholine (PCs) {34:1} $[M+K]^+$ (m/z 772.7) and {34:1} $[M+K]^+$ (m/z 798.7) were identified to be overexpressed in colon cancers at a feature selection $P<0.001$. We validated the identity of these peaks by comparing MS/MS spectra of $[M+K]^+$ ion (*m/z* 798) of PC 34:1 found on a colorectal cancer sample with those of standard PC 18:1/16:0 (Fig 3).

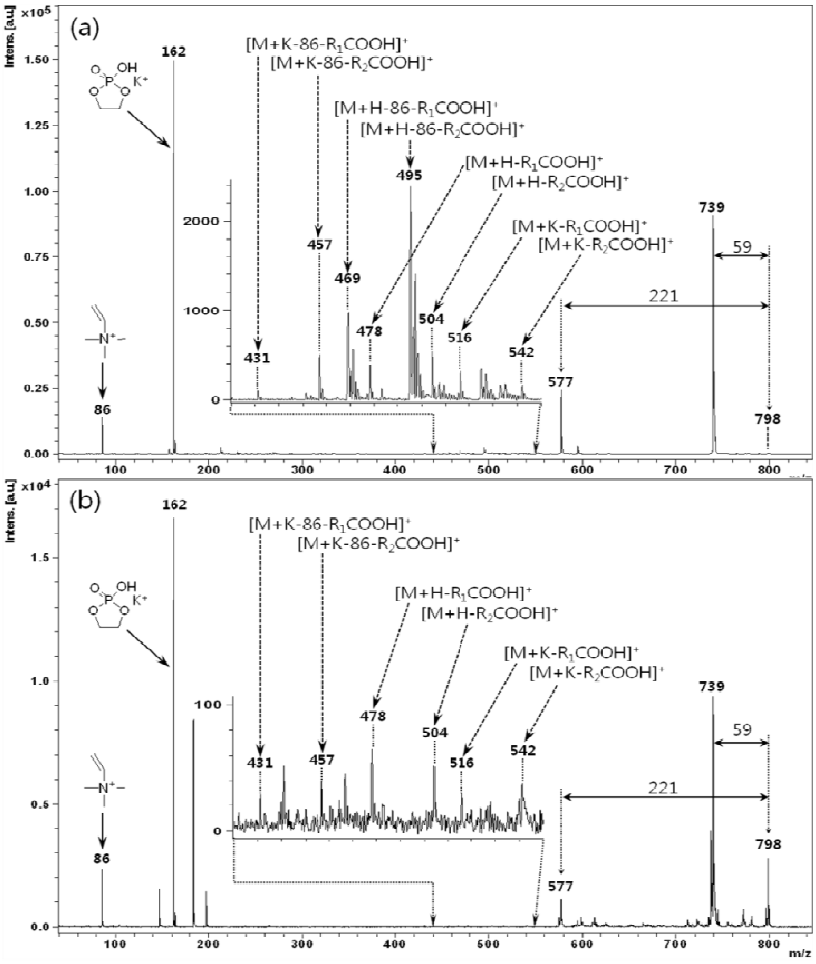

Fig 3. MS/MS spectra of (a) $[M+K]^+$ ion (*m/z* 798) of standard 1-oleoyl-2-palmitoyl-*sn*-glycero-3-phosphocholine (18:1/16:0-PC) were compared with those of (b) $[M+K]^+$ ion (*m/z* 798) of 34:1-PC species detected from a colon cancer sample [Neutral loss of m/z 59, $-NH(CH_3)_3$;221, $-PO_4K(CH_2)_2NH(CH_3)_3$].

Given encouraging results of combined lipid and protein tissue MALDI MS analysis, we extended this approach to the histology of breast and ovarian cancers. Breast cancers are different in clinical course and management according to the intrinsic subtypes (luminal, HER2, and triple-negative)[5]. We found that immunohistochemistry-defined intrinsic subtypes are different in combined lipid and protein MALDI MS profiles[6]. When class prediction analysis was performed, the median prediction accuracy for intrinsic subtype ranged from 80-81% in 100 random training-to-test partitions. Lipid profiles predicted the intrinsic subtype more accurately than protein profiles did, when tested separately.

Lipid and protein MALDI MS profiles were correlated with the histologic subypes of 23 ovarian cancers (serous, endometrioid, and clear cell). When the 0.632+ bootstrap cross validation analysis was performed on lipid MALDI MS data, permutation *P* values for cross-validated misclassification rates were less than 0.05 for the all of classifiers tested. In contrast, when the same cross validation analysis was performed on protein MALDI MS data, permutation *P* values were higher and mostly at borderline, ranging from 0.034 to 0.063. Hence, the histology distinction was attributed primarily to lipid MALDI MS profile. Interestingly, cancer-specific lipid and protein MALDI MS signatures are similar between ovarian and breast cancers. Using 7 peaks (6 lipids and 1 protein) differentially expressed between breast cancers and adjacent normal tissue samples (>2-fold, $P<10^{-5}$), principal component analysis clearly separated ovarian cancers and adjacent normal tissue samples. All peaks underexpressed in breast cancer showed coordinated underexpression in ovarian cancers, while most of the peaks overexpressed in breast cancer showed coordinated

overexpression in ovarian cancers. For example, phosphatidylcholines (PCs) {34:1} $[M+H]^+$ (m/z 760.7) and {34:1} $[M+K]^+$ (m/z 798.6) were overexpressed in both cancers.

Lipid MALDI MS profiling was useful in biomarker discovery. The MS/MS analysis identified that sulfatide (ST-OH) {42:1} $[M-H]^-$ (m/z 906.9) and phosphatidylcholine (PC) {32:0} $[M+Na]^+$ (m/z 756.7) were overexpressed in lung adenocarcinomas, compared with lung squamous cell carcinomas. Lung adenocarcinomas express a number of genes that are crucial to lung terminal differentiation and maturation, such as surfactant protein B[7]. Lung surfactant, made by type II alveolar cells, is a complex mixture composed primarily (80-90%) of phospholipids, 85% of which is phosphatidylcholine[8]. The majority of phosphatidylcholine in the pulmonary surfactant is present as dipalmitoylphosphatidylcholine (58%), containing two palmitic acids (C16:0)[9]. Hence, increase in PC {32:0} (m/z 756.7) in our lung adenocarcinoma is consistent with the tumor cell ontogeny[10].

When the spot-to-spot variation of the peak area was estimated for each of 21 normal lung tissue samples, median coefficient of variation was 21.0% (interquartile range, 13.3-36.8) for 44 peaks. Repeated measurement of 12 adenocarcinomas at one-week interval demonstrated the moderately reproducibility [median Pearson correlation, 0.95 (interquartile range, 0.94-0.98)].

3.CONCLUSIONS

Given relatively low running cost, rapid experimental procedure, and small amount of tissue required, lipid and protein tissue MALDI MS profiling approach may provide a clear advantage for the diagnosis and histology classification of common cancers. The results presented herein demonstrate that lipid and protein MALDI MS profiles may possibly complement the histopathology practice in the future.

ACKNOWLEDGEMENT

The work was supported by Converging Research Center Program through the Ministry of Education, Science and Technology of Korea (2011K000888).

REFERENCES

[1] Yanagisawa, K., Shyr, Y., Xu, B.J., Massion, P.P., Larsen, P.H., White, B.C., Roberts, J.R., Edgerton, M., Gonzalez, A., Nadaf, S., Moore, J.H., Caprioli, R.M., and Carbone, D.P., "Proteomic patterns of tumour subsets in non-small-cell lung cancer." Lancet 362(9382), 433-439 (2003).

[2] Shanta, S.R., Zhou, L.H., Park, Y.S., Kim, Y.H., Kim, Y., and Kim, K.P., "Binary matrix for MALDI imaging mass spectrometry of phospholipids in both ion modes." Anal. Chem. 83(4), 1252-1259 (2011).

[3] Mukhopadhyay, S., and Katzenstein, A.L., "Subclassification of non-small cell lung carcinomas lacking morphologic differentiation on biopsy specimens: Utility of an immunohistochemical panel containing TTF-1, napsin A, p63, and CK5/6." Am. J. Surg. Pathol. 35(1), 15-25 (2011).

[4] Lee, G.K., Lee, H.S., Park, Y.S., Lee, J.H., Lee, S.C., Lee, J.H., Lee, S,J,, Shanta, S.R., Park, H.M., Kim, H.R., Kim, I.H., Kim, Y.H., Zo, J.I., Kim, K.P., and Kim, H.K., "Lipid MALDI profile classifies non-small cell lung cancers according to the histologic type." Lung Cancer 76(2), 197-203 (2012).

[5] Perou, C.M., Sørlie, T., Eisen, M.B., van de Rijn, M., Jeffrey, S.S., Rees, C.A., Pollack, J.R., Ross, D.T., Johnsen, H., Akslen, L.A., Fluge, O., Pergamenschikov, A., Williams, C., Zhu, S.X., Lønning, P.E., Børresen-Dale, A.L., Brown, P.O., and Botstein, D., "Molecular portraits of human breast tumours." Nature 406(6797), 747-752 (2000).

[6] Hilvo, M., Denkert, C., Lehtinen, L., Muller, B., Brockmoller, S., Seppanen-Laakso, T., Budczies, J., Bucher, E., Yetukuri, L., Castillo, S., Berg, E., Nygren, H., Sysi-Aho, M., Griffin, J.L., Fiehn, O., Loibl, S., Richter-Ehrenstein, C., Radke, C., Hyotylainen, T., Kallioniemi, O., Iljin, K., and Oresic, M., "Novel theragnostic opportunities offered by characterization of altered membrane lipid metabolism in breast cancer progression." Cancer Res. 71(9), 3236-3245 (2011).

[7] Khoor, A., Whitsett, J.A., Stahlman, M.T., Olson, S.J., and Cagle, P.T., "Utility of surfactant protein B precursor and thyroid transcription factor 1 in differentiating adenocarcinoma of the lung from malignant mesothelioma." Human Pathol. 30(6), 695-700 (1999).
[8] Veldhuizen, R., Nag, K., Orgeig, S., and Possmayer, F., "The role of lipids in pulmonary surfactant." Biochim. Biophys. Acta. 1408, 90-108 (1998)
[9] Bernhard, W., Wang, J.Y., Tschernig, T., Tümmler, B., Hedrich, H.J., and von der Hardt, H., "Lung surfactant in a cystic fibrosis animal model: increased alveolar phospholipid pool size without altered composition and surface tension function in cftrm1HG/m1HGU mice." Thorax 52, 723-730 (1997)
[10] Berry, K.A., Li, B., Reynolds, S.D., Barkley, R.M., Gijón, M.A., Hankin, J.A., Henson, P.M., and Murphy, R.C., "MALDI imaging MS of phospholipids in the mouse lung." J. Lipid Res. 52(8), 1551-1560 (2011)